Protein Conformational Relaxation following Photodissociation of CO from Carbonmonoxymyoglobin: Picosecond Circular Dichroism and Absorption Studies†

Xiaoliang Xie and John D. Simon*
Department of Chemistry, University of California at San Diego, La Jolla, California 92093
Received July 9, 1990; Revised Manuscript Received November 5, 1990

ABSTRACT: Picosecond time-resolved polarization spectroscopy is used to study relaxation dynamics in myoglobin following photoelimination of CO from carbonmonoxymyoglobin. Evolution of the transient circular dichroism signal of the N band of myoglobin (probed at 355 nm) to that characteristic of equilibrium myoglobin requires ≈300 ps. This time scale is significantly longer than that corresponding to the photoinitiated bond cleavage. Transient linear dichroism of the Soret band and picosecond time-resolved magnetic circular dichroism measurements of the Q band demonstrate that the circular dichroism kinetics do not result from either time-dependent changes in the orientation of the transition moments of the heme ring or the doming of the heme that accompanies the out-of-plane motion of the iron. Finally, transient absorption data of the near-IR optical transition of photogenerated myoglobin suggest that the circular dichroism data are not a measure of the tilting of the proximal histidine. The circular dichroism data are discussed in terms of a relaxation in the tertiary structure of the protein following dissociation.

Myoglobin (Mb) is a 153 amino acid protein that serves as a reversible oxygen carrier within muscles of vertebrates. The iron-containing heme group, iron(II) protoporphyrin IX, is at the active site. The heme is bound to the protein backbone through a covalent bond between the iron and the proximal histidine (F8). On the side of the heme where the ligand is bound is another histidine, the distal histidine (E7), which is close to the iron but not bound to it. The structure of Mb is one of the most carefully characterized among all proteins. Its X-ray structure has been refined to a 1.5-Å resolution (Kuriyan, 1986) since first determined by Kendrew et al. (1960).

Pioneered by Gibson (1956), photodissociation studies of Mb and hemoglobin (Hb) have contributed immensely to our understanding of the ligand-binding processes of these proteins. In the past decade, the development of new ultrafast laser technology has led to increased efforts along these lines. Subpicosecond time-resolved UV–visible absorption (Greene et al., 1978; Jongeward et al., 1988; Martin et al., 1983), resonance Raman (Dasgupta et al., 1985; Findsen et al., 1985; Petrich et al., 1987; Terner et al., 1980), and IR spectroscopy (Moore et al., 1988) have been used to study these systems. An overview of these studies has recently been reported by Hochstrasser and Johnson (1988).

The current picture of ligated Mb photodissociation can be summarized as follows: upon photoexcitation of the liganded heme, the dissociation of the ligand is extremely fast. The absorption spectrum of ground-state Mb appears within 350 fs (Martin et al., 1983). This is followed by a vibrational cooling of the heme, with the excess heat flowing from the heme into the protein matrix within 20 ps (Genberg et al., 1987, 1989; Henry et al., 1986; Petrich et al., 1987). Ligands such as O_2, NO, and isocyanide undergo considerable geminate recombination within the first few hundred of picoseconds. There is essentially no geminate recombination in the case of CO (Henry et al., 1983) as the activation barrier for CO rebinding is considerably higher than that of the other small ligands. The dissociated CO, after diffusing out of the protein, undergoes a bimolecular binding process that occurs on a millisecond time scale (Duddell et al., 1979; Friedman & Lyons, 1980; Alpert et al., 1979; Chernoff et al., 1980).

However, the time scale of protein relaxation associated with photodissociation is not known. The currently used transient spectroscopies, infrared, Raman, and UV–visible absorption, are sensitive to heme–ligand binding but are generally less sensitive to the protein structural changes that follow photodissociation. The objective of the present work is to use time-resolved circular dichroism (CD) spectroscopy to determine the time scale on which protein relaxation occurs following ligand loss.

It is believed that conformational fluctuations of Mb play an important role in enabling the protein to carry out its biological function. For example, it has been shown that it is virtually impossible for the ligand to diffuse from the solvent into the binding site if the protein backbone is fixed at the crystallographic coordinates (Brooks et al., 1988). Molecular dynamics simulations by Case and Karplus (1979) suggest that conformational fluctuations open up the channels needed for ligand binding.

One method for studying the dynamic motions of a protein is to perturb the protein from equilibrium and then follow the ensuing relaxation. As long as the protein relaxation dynamics are longer than hundreds of femtoseconds, ultrafast photodissociation of ligands bound to the heme group provides such an approach. In the present study, we concentrate on observing only protein conformational relaxation; thus carbonmonoxymyoglobin (MbCO) was chosen as in this case complications that could arise from geminate rebinding on the picosecond and nanosecond time scales are eliminated.

As shown schematically in Figure 1, on the basis of the different crystal structures of MbCO and Mb, several structural changes are expected to take place following ligand loss. These include the movement of the iron out of the heme plane, the doming of the heme, the tilting of the proximal histidine, and a displacement of the protein backbone (shown only for the nearby F-helix in Figure 1). It is possible that the structural changes of the heme group are very fast, i.e., subpicosecond; however, it is hard to imagine that the globular

†This work is supported by National Institutes of Health Grant GM-41942 and the MMFEL Program administered by the Office of Naval Research.

0006-2960/91/0430-3682$02.50/0

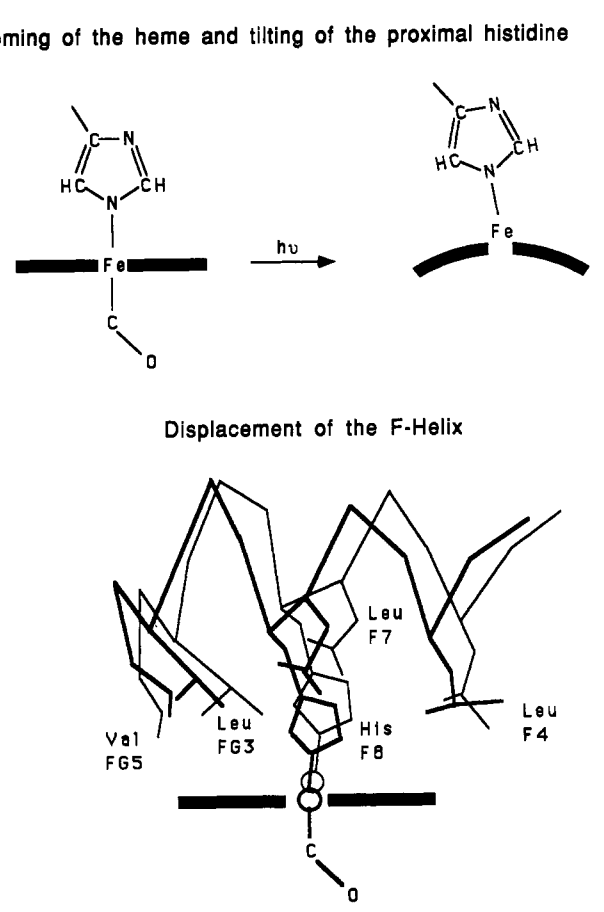

FIGURE 1: Structural changes in the vicinity of the heme ring that occur upon ligand photodissociation. In going from the six-coordinate to five-coordinate heme, the iron moves out of the heme plane, the heme domes, and the proximal histidine tilts, causing a displacement of the F-helix. There are additional changes in the tertiary protein structure that are not shown.

structue change of the protein occurs on the same time scale as photodissociation. In this paper, time-resolved picosecond CD spectroscopy is used to provide information about the conformational relaxation in photogenerated Mb.

In addition to time-resolved CD studies, a series of other time-resolved experiments aimed at characterizing conformational changes are described. In particular, picosecond time-resolved near-IR absorption and MCD measurements of the Q band are reported that address the time scales associated with the tilting of the proximal histidine and the change of the spin state of the iron, respectively. Transient absorption studies of the Q band and linear dichroism measurements of the Soret band are also presented. These related studies show that time-resolved CD spectroscopy yields information that is complementary to that obtained by using more conventional picosecond spectroscopic techniques. In particular, transient CD spectroscopy reveals a relaxation process that these other techniques cannot observe. Combining the results from this collection of experimental techniques leads to new insights into the time scales of conformational relaxation in photogenerated Mb.

Electronic States of Mb and MbCO. In this section, a brief review of the electronic transitions of Mb and MbCO is given. This discussion provides necessary background information for understanding the experiments described in the following sections.

The room temperature absorption spectra of Mb and MbCO have been extensively studied (Iizuka et al., 1974; Eaton & Hofrichter, 1981). Common features of these spectra are the Soret band (or B band) at 410–430 nm with an extinction

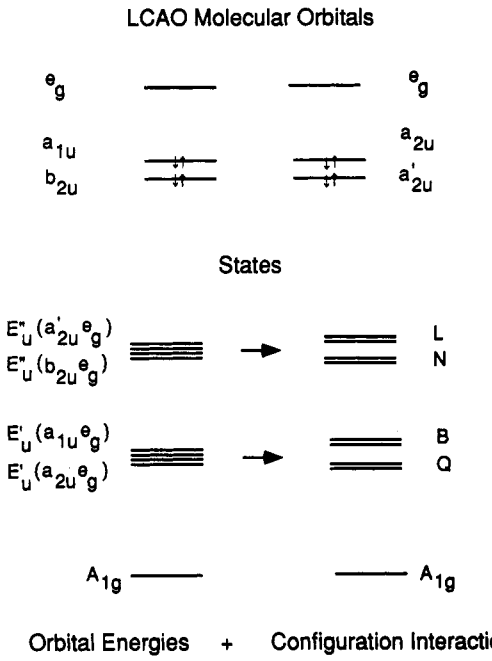

FIGURE 2: Energy level diagram for the molecular orbitals of the heme.

coefficient on the order of 10^5 cm^{-1} M^{-1}, the N band centered at 350 nm with $\epsilon \approx 4 \times 10^4$ cm^{-1} M^{-1}, and the Q band in the 520–610-nm region with $\epsilon \approx 10^4$ cm^{-1} M^{-1}. All three transitions are $\pi \rightarrow \pi^*$ transitions centered at the porphyrin ring.

A well-accepted description of these $\pi \rightarrow \pi^*$ transitions is obtained from a Hückel linear combination of atomic orbitals (LCAO) molecular orbital theory (Gouterman, 1961, 1978). In this theory, molecular orbitals are constructed by linear combinations of 24 p_z orbitals of the heme skeleton atoms. As shown in Figure 2, the four highest occupied orbitals are two closely lying pairs of orbitals, denoted $a_{2u}a_{1u}$ and $a'_{2u}b_{2u}$ in D_{4h} notation, while the lowest unoccupied orbitals are degenerate e_g orbitals. Excitation of an electron from a_{2u} or a_{1u} to e_g leads to an excited configuration ($a_{2u}e_g$ or $a_{1u}e_g$). Because these configurations have the same symmetry, they are strongly mixed by configurational interaction, resulting in two doubly degenerate B and Q states. The transition moments for excitation to the individual excited configurations add to give a very large net transition moment for the higher frequency B band but subtract and nearly cancel for the lower frequency Q band. This accounts for the difference in oscillator strengths of the B and Q bands.

Similarly, the N band and L band arise from an interaction between the configurations generated by the $a'_{2u} \rightarrow e_g$ and $b_{2u} \rightarrow e_g$ excitations, respectively. The L band in Mb is buried under the protein absorption at a wavelength shorter than 300 nm. This feature is not relevant to the present work. The N band appears at 350 nm. The N, B, and Q states are all singlets, and all lie much higher in energy than the ligand field states that lead to photodissociation of the iron–ligand bond (Greene et al., 1978).

The unique feature of the Q band is that it shows vibrational structure. There are two distinct Q bands. The lower frequency band, Q_0, corresponds to excitation to the ground vibrational level of the Q state, while the higher frequency band, Q_v, corresponds to excitation to a series of upper vibrational levels of the Q state. The Q_0 and Q_v bands of MbCO are located at 568 and 538 nm, respectively. For Mb, the Q_0 band appears as a shoulder on the Q_v band at 556 nm. The B band has essentially no vibrational structure except in the case of MbCO where there is a small shoulder at 400 nm that

has been assigned to the Frank–Condon activity of this transition. The enormous vibrational structure of the Q band, however, has been attributed to vibronic borrowing from the intense B band through Hertzberg–Teller coupling (Perrin et al., 1969).

The presence of a 4-fold rotation axis of the heme results in a constraint on the possible directions of transition dipole moments: the transitions are either polarized parallel to the 4-fold axis (defined as the z axis) or polarized equally in all directions perpendicular to the 4-fold axis (x,y polarized). The N, B, and Q bands are all doubly degenerate, x,y-polarized transitions. The transition dipole moments of the two double degenerate states are perpendicular to each other but have no preferred directions in the heme plane. This is due to the fact that any linear combination of the two degenerate states results in another set of degenerate transitions perpendicular to each other but rotated with respect to that of the original states considered. With respect to these transitions, the heme is considered a circular absorber.

In reality, the protein matrix removes the exact 4-fold symmetry of the heme, resulting in a lifting of the degeneracy of the e_g orbitals and thus a splitting of the degeneracies of the N, B, and Q bands. There are several possible causes of the splitting, including the Jahn–Teller effect (Sutherland, 1971), the existence of two vinyl side chains on the heme, doming or ruffling of the heme, the nonbonded interaction of the planar proximal histidine with the heme (Olafson & Goddard 1977; Rohmer et al., 1987), a nonlinear iron–ligand bond (Bolard, 1972), and/or structural restraints imposed on the heme by the noncovalent forces of the protein. According to molecular orbital theory, the two split transitions should have slightly different oscillator strength. Eaton and Hofrichter (1981) have determined the splitting of the B and Q bands by conducting polarized absorption measurements on single crystals of many heme protein derivatives. The small splitting of the Soret band is visible with only a few techniques. The splitting of Q_0, however, is obvious and appears even in the solution absorption spectrum of MbCO at room temperature.

In the above discussion, only $\pi \rightarrow \pi^*$ transitions are considered; however, the d orbitals of iron perturb the porphyrin transitions. In MbCO and other ferrous six-coordinated complexes, the Fe^{2+} is in a low-spin state, $S = 0$. In the five-coordinated Mb, the Fe^{2+} is in a high-spin state, $S = 2$ (a quintet state). The B band and Q band are red shifted in going from MbCO to Mb, whereas the shift of the N band is rather small.

In addition, in the presence of the crystal field generated by the four nitrogen atoms of the heme, the proximal histidine, and the distal ligand, there are several d $\rightarrow$ d transitions as well as charge-transfer transitions between the iron and the heme. These transitions have been verified both by calculations and by various spectroscopies (Eaton et al., 1978). The d $\rightarrow$ d transitions are in the visible and near-IR region. They are generally much weaker than the Q band and thus are not easily observed in the absorption spectrum. The charge-transfer bands occur in the near-IR region, also with weak intensity. Of particular importance to the present work is a distinct charge-transfer band at 758 nm for Mb. Using extended Hückel calculations and spectroscopic measurements, Eaton et al. (1978) have assigned this band to the $a_{2u}(\pi) \rightarrow d_{xy}$, porphyrin-to-iron, charge-transfer transition of the ferrous high-spin complex. Polarization measurements of single crystals show that the transition is polarized in the heme plane (Eaton & Hofrichter, 1981). Low-temperature studies also indicate that this band is a sensitive probe of the local structure of the heme through its interaction with the protein environment (Chavez et al., 1990; Frauenfelder et al., 1988). The picosecond dynamics of this band will be examined and discussed later.

Experimental Procedures

Transient Circular Dichroism Spectroscopy. The picosecond time-resolved CD spectrometer has been described in detail elsewhere (Xie & Simon, 1989; Xie, 1990). Briefly, a mode-locked, Q-switched, and cavity-dumped YAG laser (Xie & Simon, 1988) provides high-energy IR pulses at repetition rates up to 1 kHz. These pulses are frequency doubled by a CD*A crystal (pump pulses) and tripled in KDP (probe pulses). The 532-nm pulses are attenuated to 60 μJ/pulse, passed down an optical delay line through a depolarizer and a rotating half-wave plate, and then focused onto a spinning sample cell. The beam waist at the focal point is $\approx$0.4 mm. To examine the dynamics of the N band, a weak probe beam at 355 nm is polarization modulated by a piezoelectric modulator (Hinds International Model PEM-80) that is timed to the laser Q switch so that successive laser pulses alternatively pass through the modulator when $+\lambda/4$ and $-\lambda/4$ voltage is being applied. The transmitted probe beam is detected by a head-on PMT (Hamamatsu Model 1398). The output of the PMT is sent to a track-and-hold circuit and phase-sensitive detection referenced to the polarization modulation frequency is used to detect the transient CD signal. The time resolution of the experiment is $\approx$50 ps, limited by the laser pulse width.

Transient CD experiments on the B band and Q band were also carried out by using tunable dye lasers to generate the necessary probe light. In these two cases, only level changes were observed with a poor signal-to-noise ratio. The former was complicated by the large OD change accompanying photodissociation, while the latter suffered from small transient signals. Further improvement of the signal-to-noise ratio is required to measure dynamics at these wavelengths.

Transient Near-IR Absorption Studies. The extinction coefficient of the near-IR band of five-coordinate Mb is $\epsilon \approx 150$ cm^{-1} M^{-1} at 60 K, 2 orders of magnitude smaller than the Soret band. This underlies the difficulty in conducting picosecond experiments on this band. With the detection scheme developed for CD measurements, time-resolved near-IR spectra of photogenerated Mb could be measured. The specific modifications of the detection system for the near-IR experiments are as follows: The mode-locked Q-switched Nd:YAG laser is used to pump two cavity-dumped dye lasers, providing pump and probe laser pulses, respectively. The lasing medium of the probe dye laser is a mixture of LDS750, LDS765, and LDS821 dyes (Exciton). The optimum concentrations and proportions were empirically determined in order to obtain a broad and structureless bandwidth from 750 to 810 nm. No tuning elements are used in the probe laser. Pump pulses of 20 μJ are generated from the second dye laser operated at 570 nm (R6G). The time resolution of the apparatus is $\approx$35 ps. Both pump and probe beams are depolarized in order to avoid linear dichroism artifacts. The transmitted probe pulses are dispersed by a scanning monochrometer (Instruments SA). The slits are adjusted to give a spectral resolution of 1 nm. The output light is detected by a PMT and processed with phase-sensitive detection. In these experiments, the lock-in amplifier is referenced to the frequency of an optical chopper in the pump beam.

Transient Q-Band Absorption Studies. For Q-band transient absorption experiments, excitation pulses (80 ps FWHM) are generated from the second harmonic of the cavity-dumped

YAG output. These pulses are attenuated to 25 μJ/pulse, modulated by a mechanical chopper, and focused into the sample with a beam waist of ≈0.4 mm. The pump power thus obtained (200 MW/cm²) is significantly lower than that used in previous picosecond experiments on heme photolysis reactions. In addition, we found that the polarization of the pump and probe beams is crucial in accurately detecting transient signals. In order to avoid coherent artifacts near zero delay time, the pump and probe beams need to be depolarized. This issue will be discussed in detail later. In practice, both pump and probe pulses are passed through a depolarizer or a quarter-wave plate. In addition, a rotating half-wave plate in the pump beam is used to randomize any residual polarization. The probe pulses are generated by using a cavity-dumped dye laser that is pumped by the Q-switched, mode-locked, and cavity-dumped YAG laser. When no intracavity tuning element is used, the bandwidth of the dye laser is about 10 nm (R6G). Adding a birefringent filter (Coherent) into the cavity does not decrease the bandwidth but allows the center frequency of the band to be tuned. A subtractive double monochrometer (Spex) is used to subsequently disperse the colors of the laser pulses without broadening their temporal width. In this manner, pulses are easily tuned from 560 to 600 nm with a 1-nm resolution. The detection system is similar to that described above.

Transient Magnetic Circular Dichroism Measurements of the Q Band. A detailed description of the modifications needed to record picosecond MCD data can be found elsewhere (Xie & Simon, 1990). The external magnetic field was provided by a 4000-G permanent magnet (Jasco Model PM-1) that was intensified to 8000 G by magnetic shimming of the gap between two poles. The direction of the magnetic field was parallel to the probe beam. The pump and probe beams pass through 7-mm holes drilled through the two poles; a flowing sample cell is placed inside the gap and translated back and fourth by a motorized stage during experimental runs. Transient MCD experiments were carried out on the Q band and Mb. The pump and probe beams were generated as described in the above section on the details of collecting transient absorption data on the Q band.

Transient Linear Dichroism Measurements. Slight modifications (modulation voltage and timing) of the CD apparatus enables detection of picosecond linear dichroism signals. Pulses from a R6G dye (570 nm) and attenuated to 2 μJ/pulse and used for excitation. A weak polarization-modulated probe beam is derived from the frequency-doubled output of the second dye laser (LDS821 dye). The time resolution of the experiment is ≈35 ps.

Sample Preparation. Horse metMb was purchased from Sigma. The pH 7.0 Tris-bis buffer solution of MbCO was prepared under strict anaerobic conditions according to a previously published procedure (Samejima & Yang, 1964). Except for the MCD experiments in which a flow cell is used, a total volume of 1.5 mL of sample is sealed in a home-made rotating sample cell with a 2-mm path length. The Mb concentration was ≈0.8 mM, with optical densities of 1.7 at 532 nm and >4 at 355 nm. Under these conditions, a pump pulse of 60 μJ (CD and MCD experiments) excites more than 90% of the sample in the volume interrogated by the probe pulses.

Results and Discussion

Time-Resolved CD Experiments. There have been many steady-state CD studies of heme proteins (Myer & Pande, 1978; Woody, 1978). The CD of Mb and MbCO between 300 and 600 nm is predominantly due to the N-, B-, and Q-band transitions of the heme. The heme itself is achiral and is thus optically inactive. The optical activity of the heme transitions arises from the asymmetrical protein environment. A time-resolved CD measurement would provide valuable information on the restructuring of the surrounding asymmetric environment following ligand loss.

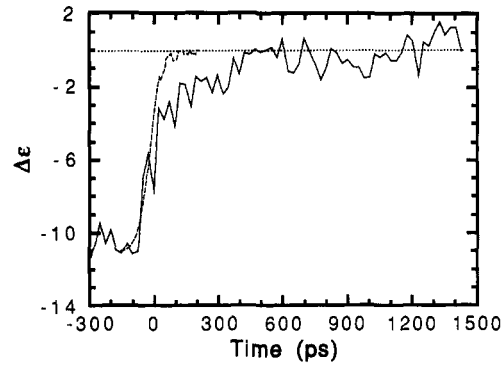

FIGURE 3: Transient circular dichroism kinetics of Mb probed at 355 nm following the photodissociation of CO (solid line). The dashed line is the normalized transient absorption signal recorded at this wavelength. The transient CD data reveal two processes. The dotted line is the equilibrium CD value for Mb. The instantaneous component (≈60% of the change in signal) is due to the electronic state change that occurs upon photodissociation. The longer relaxation time reflects conformational changes in the surrounding protein structure.

Toward this goal, Kliger and co-workers reported nanosecond time-resolved CD data for the photodissociation of CO from MbCO (Milder et al., 1988). Upon photolysis, the CD signal changes from that expected for MbCO to that of Mb within the time resolution of the experiment. No further change in signal is observed over a time scale of hundreds of nanoseconds. These data indicate that the protein relaxation occurs on the subnanosecond time scale.

In Figure 3, picosecond time-resolved CD kinetics for the N band of Mb are plotted as a function of time with respect to photolysis. The dashed line is a normalized transient absorption run of the same sample at the same wavelength, providing a measure of the instrumental response function.

The level change of the CD signal from $\Delta\epsilon \approx -12$ to $\Delta\epsilon = 0$ is consistent with previously reported steady-state CD values of MbCO and Mb at this wavelength (Milder et al., 1988). However, the CD kinetics are distinctly different from the transient absorption study. There is a fast initial rise within the instrumental response time, followed by a slower rise that reaches zero at about 300–400 ps. It is important to note that both Mb and MbCO have a large absorption at 355 nm (the N band for both species is centered at 350 nm, with Mb having a slightly larger extinction coefficient). Our data suggest that, upon photodissociation, the photogenerated Mb gains oscillator strength immediately, but the absorption difference between left and right circular light decays to zero gradually. This is confirmed by experiments conducted with both unligated Mb and achiral dye molecules. In both cases, no CD signal is observed at any time. These experiments demonstrate that the evolution of the CD signal observed in the photolysis of MbCO does not arise from a thermal heating of the protein following photolysis or any coherent effects between the pump and probe laser beams.

The N band is clearly sensitive to ligand binding. Thus, even if there were no conformational changes upon photodissociation, CD changes in this region would be observed upon ligand detachment due to the change in the electronic structure of the heme. We attribute the fast rise in the CD signal to the electronic structure change of the heme. The second component reveals a new relaxation process that is 2 orders of magnitude longer than that for photodissociation. The

remainder of this paper examines the nature of this relaxation process.

Theoretical calculations of the CD spectra of Mb (and Hb) based on the known three-dimensional structure were first reported by Hsu and Woody (1971). This work established that the origin of the optical activity for heme transitions arose from a coupled oscillator interaction between the $\pi \rightarrow \pi^*$ transitions on the heme and those of the surrounding aromatic side chains. Various other possible mechanisms (Woody, 1978) could also contribute to the CD, including distortion of the porphyrin (i.e., nonplanarity of the heme), the one-electron mechanism (Mason, 1979), and the gaining of magnetic dipole character by mixing of $\pi \rightarrow \pi^*$ transitions with $d \rightarrow d$ transitions. Hsu and Woody (1971) showed that coupled oscillator interactions could account for both the sign and magnitude of the observed CD bands in Mb. These calculations also indicated that aromatic residues as far as 12 Å away from the heme contribute appreciably to the CD spectrum.

These calculations are based on Tinoco's extension (Tinoco, 1962) of Kirkwood's theory (Kirkwood, 1937). The underlying assumption of Kirkwood's theory is that the molecule can be divided into N smaller groups where there is no charge transfer between the various groups. The rotational strength R for an electrically allowed, magnetically forbidden heme transition, coupled with electrically allowed transitions of surrounding aromatic residues, is given by

$$R_{x,y} = -\frac{2\pi}{c}\sum_i \frac{V_{xi,yi}\nu_{x,y}\nu_i \vec{r}_{xi,yi} \cdot \vec{\mu}_i \times \vec{\mu}_{x,y}}{h(\nu_i^2 - \nu_{x,y}^2)} \quad (1)$$

$$R = R_x + R_y \quad (2)$$

where the summation is over all the electrically allowed $\pi \rightarrow \pi^*$ transitions of the aromatic residues, μ_i and $\mu_{x,y}$ are the transition dipole moments for the ith $\pi \rightarrow \pi^*$ transition of the aromatic residues, and x and y represent the two degenerate transitions of the heme. The corresponding transition frequencies are ν_i and $\nu_{x,y}$, respectively. The transition dipole moments and the transition frequencies can be obtained from either spectroscopic measurements or molecular orbital calculations. $V_{xi,yi}$ is the interaction potential between the transition dipole moment of the heme and that of the ith transition of the aromatic residues. Under a point monopole approximation (Hsu & Woody, 1971; Tinoco, 1962) $V_{xi,yi}$ can be calculated with knowledge of the wave functions of the two molecular states involved. The distances between the centers of the heme and the aromatic side chains, $r_{xi,yi}$, are easily obtained from X-ray structure data.

The aromatic amino acids that contribute to the optical activity of the heme are shown in Figure 4. The contribution of each of these aromatic residues to the rotational strength of the various heme $\pi \rightarrow \pi^*$ transitions has been tabulated by Hsu and Woody (1971). The sum of the rotational strengths for the doubly degenerate transitions, $R_x + R_y$, gives the total rotational strength of a particular band. In a coupled oscillator model, the individual contributions of each residue are additive. The dominant contributions come from interaction between the heme and Phe(33,14B), Phe(43,1CD), Tyr(103,4G), and Tyr(146,23H). Interactions with the proximal and distal histidines, His(93,8F) and His(64,7E), respectively, are much smaller. The latter can be rationalized by realizing that these two histidines have relatively symmetrical (achiral) orientations with respect to the heme.

The near degeneracy of the N, B, and Q band adds further sensitivity to the CD spectrum. R_x and R_y have different signs

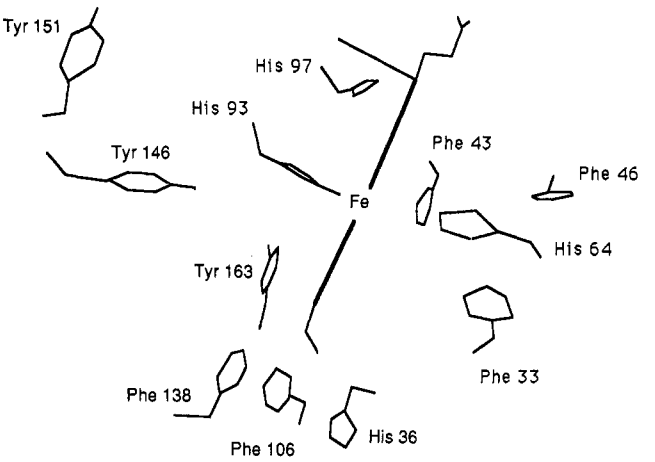

FIGURE 4: Orientations of the amino acids responsible for the CD spectrum of the heme group in Mb in the UV–visible spectral region [from Hsu (1970)].

and similar magnitudes and, to a large extent, often cancel each other (Hsu & Woody, 1971; Hsu, 1970). The magnitude of R_x or R_y is determined by the direction of the transition dipole and varies if the transition dipole rotates in the heme plane. As discussed in the previous section, the two perpendicular transition dipoles of the doubly degenerate band have no preferred direction if the heme has D_{4h} or C_{4v} symmetry. It turns out that the total R is independent of the direction of the x and y transitions assumed in the calculations (Hsu, 1970). The lifting of the degeneracy in Mb, however, makes the heme an elliptical absorber in which the transition dipole moments have well-defined directions (the short and long axis of the ellipse). The directions of transition dipole moments for Mb have not been experimentally measured. The consequence of this nondegeneracy on the CD spectrum is that the shape of the CD bands depends on the orientation of the these transition dipole moments (Hsu & Woody, 1971). It is still true that the total integrated area under the CD curve of a particular band is a constant for all possible orientations of the transition dipoles.

As indicated by eq 1, CD is determined by the relative orientations of the transition dipole moments of the heme and the aromatic side chains. Since the crystallographic data reveal a protein structural difference between Mb and MbCO, one would envision that photogenerated Mb would first have the conformation of MbCO, which then relaxes to that of Mb. In light of eq 1, this relaxation should appear as a time-dependent change in the CD signal of the heme transitions. It is important to note that even though a localized heme transition is detected, the tertiary structure of the protein is actually probed through the coupling with the aromatic residues.

If coupled oscillator interactions are the sole origin of CD, the data shown in Figure 3 suggest that the tertiary structure of the protein requires several hundred picoseconds to fully relax to the equilibrium deligated structure. However, to prove this conclusion, one must carefully consider other molecular mechanisms (in addition to tertiary relaxation) that could lead to a dynamic evolution in the CD signal. In particular, there are two potential explanations that need to be addressed.

First of all, the signal could be due to an orientational change of the two heme transition dipole moments. This would result in a change of R according to eq 1. This effect can result from either a displacement of the heme or a rotation of the transition dipoles within the heme. The importance of this process can be elucidated by carrying out transient linear dichroism experiments. The results from such studies are discussed in a later section.

The second mechanism that needs to be considered involves a dynamic lifting of the degeneracy of the N band. This can lead to a time-dependent change in the shape of the CD band, which can appear as a kinetic process in a CD experiment performed at a single wavelength. As the Q band is most sensitive to the splitting of the e_{2g} orbitals, the possible importance of this process can be determined by performing careful transient absorption measurements of the Q band. The results are discussed in the next section. Time-resolved MCD measurements can provide information complementary to the Q-band absorption studies. These results are discussed in a later section. It is worth pointing out that the observed CD kinetics are most likely due to a vanishing of rotational strength rather than shape changes of the CD band. This is consistent with the steady-state data in which the rotational strength for the N band of equilibrated Mb is small compared to that of MbCO (Milder et al., 1988).

Finally, there are other possible origins of heme optical activity, in addition to coupled oscillator interactions, that cannot be ignored. The two vinyl side chains and the doming of the heme in the Mb structure induce intrinsic chirality to the heme. CD calculations (Woody, 1978) on distorted protoporphyrin IX show that twisting of the 2- and 4-vinyl groups out of the heme plane has a profound effect on the rotational strength [The X-ray structure shows the vinyl groups are pointed out of the heme plane in Mb; Kuriyan (1986)]. The doming of the heme in Mb, as observed from the X-ray structure, also leads to a substantial calculated rotational strength. Recently, there has been an experimental report that casts doubts on the conclusion that the coupled oscillator mechanism is the sole origin of heme optical activity (Aojula et al., 1988). The introduction of heme into apomyoglobin produces a reconstituted heme protein that contains a mixture of two isomers (La Mar et al., 1983). One of these isomers is the same as native Mb; the other one differs in that the heme is rotated 180° about the α–γ–meso axis. The effect of this rotation is that the positions of the two carboxy groups are interchanged and the two vinyl groups point in opposite directions. This disordered form can be distinguished from the native protein by using NMR spectroscopy. It is thermodynamically unstable and converts to the native form during the course of a few hours. A CD study showed that the rotational strength of the Soret band for a 50% mixture of the two forms is reduced by almost half compared to the native structure (Aojula et al., 1988). This change might not be accounted for by a coupled oscillator mechanism—induced chirality of the porphyrin may be involved (R. Woody, personal communication). Therefore, a dynamic distortion of the heme structure following photodissociation could also be responsible for the observed CD kinetics. Thus, distortion of the heme can result in CD changes not only through lifting of the degeneracy but also by introducing intrinsic asymmetry to the heme.

Potentially, time-resolved resonance Raman spectroscopy can observe such heme structure changes. Unfortunately, recent reports have not yielded consistent experimental evidence concerning structural evolution from the picosecond-to-nanosecond time regime. For MbCO photolysis, Findsen et al. (1985) reported that the iron–histidine stretching frequency reaches its equilibrium value within 30 ps, whereas Dasgupta et al. (1985) reported that the core marker bands are shifted at 30 ps. Recently, Alden et al. (1990) have studied the power-dependent behavior of the resonance Raman spectra of deoxy-Hb and concluded that the time-resolved resonance Raman experiments can be complicated by a nonlinear scattering process induced by strong resonant laser flux.

The major objective of the various spectroscopic experiments described in the following sections is to establish whether structural or electronic distortions of the heme are responsible for the observed CD change. For example, since vinyl groups have a large influence on the conjugated π-electron system, motions of these groups might be sensed by careful transient absorption measurement of a heme $\pi \rightarrow \pi^*$ transition. Although femtosecond transient absorption work (Martin et al., 1983) and MD simulations (Henry et al., 1985) indicate that the displacement of iron and the doming of the heme are complete within 1 ps, it is possible that a subsequent small time-dependent distortion of the heme might be responsible for the CD kinetics. The near-IR and Q-band absorption studies and the MCD experiments on the Q band discussed below confirm that the temporal evolution of the CD signal does not arise from structural or electronic changes of the heme.

Transient Absorption Studies of the Q Band. Picosecond transient absorption spectra of the Q band of Mb following photodissociation of MbCO were first recorded by Greene et al. (1978). Since then, there have been few experiments that have carefully monitored the evolution of this spectral feature. We have examined the dynamics of this band for two major reasons. First, the Q_0 band is the most sensitive optical transition to the lifting of the degeneracy of the e_{2g} orbitals; the splitting of Q_{0x} and Q_{0y} can be seen in the room temperature absorption spectrum. This is important, for as discussed above, a dynamic change in this degeneracy might account for the CD kinetics observed. Second, picosecond resonance Raman work on the core marker band indicates an unrelaxed heme structure at 30 ps (Greene et al., 1978). Resonance with the Q band was used to obtain this spectrum, and the observation of a Raman shift at 30 ps implies that the optical spectrum might be different as well.

Many transient absorption studies, ranging from nanoseconds to femtoseconds, have been reported on the Soret band for the photodissociation of CO from MbCO (Hochstrasser & Johnson, 1988). The difference spectra recorded after photolysis and a nanosecond pulse are identical with the steady-state difference spectra. Most picosecond and subpicosecond spectra, however, are slightly different from those observed at steady state. Whether these subtle changes are due to structural intermediates or experimental artifacts still remains to be answered. Potential experimental complications include multiphoton excitation and coherence effects. Recently, Janes et al. (1988) have commented on the need to carefully monitor the evolution of these spectra between the picosecond and nanosecond time regimes. Their results showed that the Soret band difference spectrum remains stationary from 30 ps to 6.5 ns.

Figure 5 shows the transient difference spectra of the Q band for Mb at a 0-ps, 1-ns, and 10-ns time delay. Within experimental error, the position of the isosbestic points, maxima, and minima are time independent. The observation that there is no spectral evolution suggests that the heme structural changes probed by the Q band are also completed within the instrumental response time of 35 ps. This is not consistent with the Q-band resonance Raman work (Dasgupta et al., (1985). Unfortunately, it is not clear how large a spectral shift in the Q band should be observed if there is a dynamic splitting of the electronic transitions. Given the large width of this absorption feature, it is possible that a small shift could be masked. However, in conjunction with the transient linear dichroism measurements presented below, these data

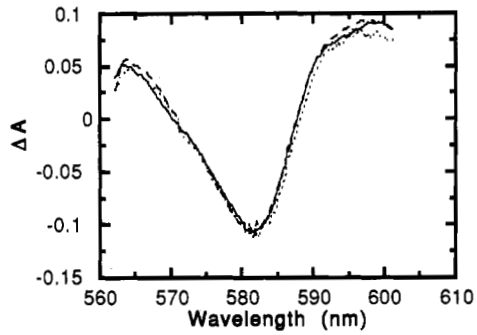

FIGURE 5: Transient difference spectra of the Q_0 band following photodissociation of MbCO with a 0-ps (solid line), 1-ns (dotted line), and 10-ns (dashed line) time delay taken with a 35-ps instrumental response time. No spectral evolution is observed between 35 ps and 60 ns.

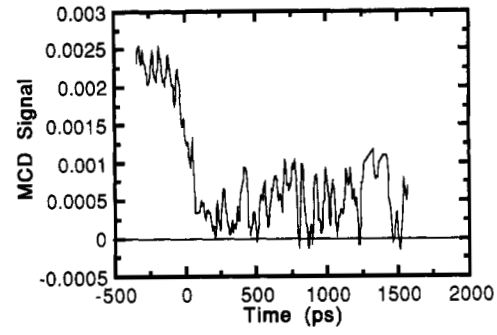

FIGURE 6: Time-resolved MCD signal at 580 nm following the photodissociation of MbCO at 532 nm. At $t = 0$, the signal drops from that characteristic of a low-spin iron to that reflective of a high-spin metal. The signal is constant for the following nanosecond. These data suggest that there are no dynamical changes in the structure of the heme on this time scale.

support the conclusion that the observed CD kinetics are not due to either a dynamic splitting of the porphyrin e_g orbitals or distortions of the heme structure in response to photolysis.

Picosecond MCD Studies. Magnetic circular dichroism (MCD) is a sensitive spectroscopic tool that can provide detailed information on the electronic structure of molecular systems (Buckingham & Stephens, 1966; Goldbeck, 1988; Holmquist, 1978; Schatz & McCaffery, 1969; Sutherland & Holmquist, 1980; Vikery, 1978). In MCD spectroscopy, the absorption difference of left and right circular polarized light of a sample in an external magnetic field is measured. Recently, Kliger and co-workers reported nanosecond time resolution in measuring MCD signals (Goldbeck et al., 1989; Woodruff et al., 1990). We have recently reported a technique for measuring MCD signals on the picosecond time scale (Xie & Simon, 1990).

For metal porphyrins, the shape and intensity of the MCD spectrum are sensitive probes of the spin state of the metal as well as the detailed electronic structure of the heme (Vickery et al., 1976). This feature has been exploited in determining the spins of metal ions in ground-state biological systems as well as in transient intermediates on the nanosecond and longer time scale (Woodruff et al., 1990).

In this section, a picosecond time-resolved MCD study of the Q_0 band of Mb following the photoelimination of CO is examined. There have been several steady-state MCD studies of Mb and related systems (Bolard & Garnier, 1972; Kajiyoshi & Anon, 1975; Springall et al., 1976). The Q-band transition of porphyrins coordinated to a low-spin metal and D_{4h} symmetry is believed to have A-type MCD spectra (Holmquist, 1978; Sutherland & Holmquist, 1980). Previous studies show that the MCD spectrum of the Q_0 band is sensitive to the spin state of the central metal ion and its axial ligation (Sharanov et al., 1978; Vickery et al., 1976). Thus, a picosecond time-resolved measurement will enable one to determine information concerning the time scale associated with the change in spin of the coordinated iron and the motion of the iron atom out of the heme plane.

The time-dependent MCD change at 580 nm following photodissociation of MbCO is shown in Figure 6. The CD signal drops to near zero within the instrumental response time. The level change is expected given the steady-state MCD signals of Mb and MbCO at this wavelength (Bolard & Gernier, 1972). Unfortunately, because of the small magnitude of the MCD signal for Mb in the visible region, our current signal-to-noise ratio and magnetic field strength limit our ability to determine whether or not there is any subsequent evolution of the transient MCD signal of photogenerated Mb on the picosecond time scale following the large decrease in intensity observed at zero time. The mean value of the signal for $t > 0$ is that expected for the deligated species.

The instantaneous MCD level change at 580 nm to that expected for equilibrated Mb supports the conclusion drawn from subpicosecond transient absorption studies (Martin et al., 1983) that the spin change of the iron occurs on the subpicosecond time scale. This MCD result also supports the conclusion that there is no detectable evolution of electronic state (or structure) of the heme from 30 ps to several nanoseconds following photodissociation.

Transient Linear Dichroism Measurements. Time-resolved linear dichroism is a valuable experimental technique for studying the motions of chromophores in solution (Fleming, 1986). The underlying principle of these experiments is as follows. A linearly polarized pump beam is used so that those molecules with transition moments that have a projection on the polarization direction of the light are preferentially excited. The ensuing absorption difference in the parallel and perpendicular polarization directions (linear dichroism) is then probed as a function of time. As molecules rotate, the directions of the transition dipole moments are randomized, resulting in a vanishing of the linear dichroism signal. The linear dichroism decay reflects properties of molecular motions that rotate the direction of the transition dipole. Because both motion of excited molecules and motion of unexcited molecules contribute to the signal, the linear dichroism data are simplified when the absorption bands of the excited molecules and the ground-state unexcited molecules do not overlap. For this reason, a linear dichroism experiment on the N band, though directly relevant to the CD experiment, would be less informative than a study of the well-separated Soret bands of MbCO and Mb.

A quantitative description for a circular absorber, such as the heme, is

$$r(t) = \frac{A_{\parallel} - A_{\perp}}{A_{\parallel} + 2A_{\perp}} = 0.1\langle \mathbf{n}(0)\cdot\mathbf{n}(t)\rangle \qquad (3)$$

where the $r(t)$ is called the absorption anisotropy; $A_{\parallel}$ and $A_{\perp}$ are the absorptions of light polarized parallel and perpendicular to the polarization vector of the exciting light, respectively. The unit vector $\mathbf{n}$ represents the heme normal, and the brackets denote an assemble average. An initial absorption anisotropy of 0.1 is characteristic of a circular absorber (Magde, 1978).

The overall rotational time of Mb is about 10 ns; the linear dichroism signal should decay with this time constant. However, three possible mechanisms could lead to fast components contributing to the linear dichroism decay on the picosecond time scale. First, if probed at the Soret band of MbCO (≈420

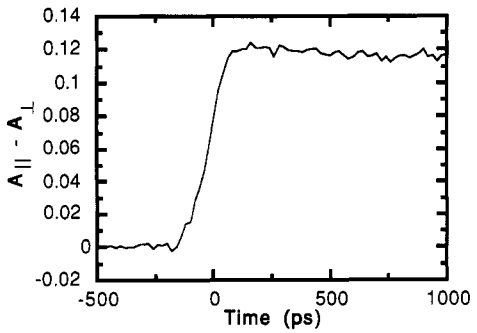

FIGURE 7: Transient linear dichroism kinetics probed at 440 nm (near the absorption maximum of Soret band of Mb). There is no fast component in the decay, indicating that neither a structural displacement of the heme nor rotation of the heme transition dipole moments is observed from 35 ps to several nanoseconds following photolysis.

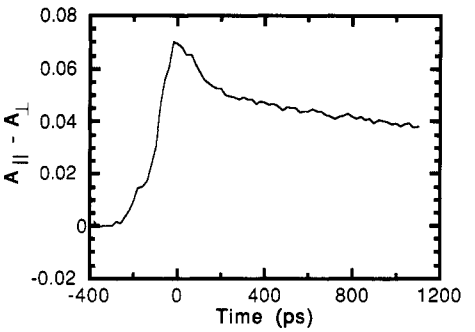

FIGURE 8: The linear dichroism signal obtained under the same conditions as in Figure 7 except that a 7-μJ pump pulse energy was used. There is an artificial signal at zero time delay due to nonlinear effects.

nm), a depolarization on a fast time scale can be a reflection of the equilibrium fluctuation of the heme normal within the fixed protein matrix. Second, if probed at the Soret band of Mb (≈440 nm), a fast depolarization can result from a displacement of the porphyrin ring after photodissociation of MbCO. For such a nonequilibrium process, eq 3 is not applicable. Finally, a fast depolarization can also result from either a rotation of the two transition dipole moments within the heme plane or a difference in the magnitudes of the two moments. When the heme is modeled as a perfect circular absorber, rotation of the two equal transition dipoles has no depolarization effect. According to the discussion above, either the heme displacement or rotation of the heme transition dipoles can give rise to a time-dependent CD change. This underlies the motivation for conducting careful linear dichroism measurement.

Figure 7 shows the linear dichroism data probed at 440 nm, a wavelength at which the absorption of MbCO is negligible. There is no noticeable fast component. These data exclude the possibility of appreciable heme displacement from 35 ps to several nanoseconds time delay after photodissociation, not a surprising conclusion considering the rigidity of the heme pocket. The data also reveal no evidence for the rotation of the heme transition dipoles on this time scale. Therefore, heme displacements and heme transition dipole rotations are not likely to be responsible for the observed CD kinetics. A linear dichroism study probing at 417 nm (data not shown) also shows no fast components. In addition, at this wavelength $r(0) = 0.1 \pm 0.05$, indicating that the fluctuations of the heme normal during the first few tens of picoseconds are limited to a very small cone (<5°).

It is important to stress that our experience indicates that an accurate measurement of linear dichroism signals for this system is a nontrivial task. In particular, power-dependent signals were commonly observed. Data plotted in Figure 7 were obtained with very low energy excitation (2 μJ/pulse). In comparison, data obtained under the same conditions except that a 7-μJ pulse energy was used are plotted in Figure 8. This pump power is far lower than that used in most previous experimental reports, yet it generates a strong artificial signal around zero time delay. The signal is similar to the known coherent artifact (Fleming, 1986), although pump and probe beams of different colors are involved. The origin of this nonlinear process remains to be explored, but its existence results in concerns about many previous picosecond transient absorption studies on heme proteins in which changes in the shape of the absorption for transient species and fast kinetic processes were often observed around zero time. The manipulation of pump–probe polarizations in previous experiments were seldom addressed; however, they are crucial to the presently discussed kinetics. It is common to use linearly polarized pump and probe beams. Setting the magic angle (54.7°) between pump and probe polarization directions eliminates the complication of photoselection to the observed kinetics, but it by no means avoids the spike-like signal at time zero as the pump and probe pulses still have parallel components. Perpendicular pump and probe polarization help to reduce this unwanted effect; however, the signal thus obtained would contain information on both level kinetics and dynamic fluctuations of the chromophore, which are not desirable either.

Our approach to overcome this difficulty is to use depolarized pump and probe pulses in all the reported transient absorption and depolarized pump light for the MCD and CD experiments. It is worth mentioning that the Q-band difference spectra at zero time delay obtained by using a linearly polarized pump beam were significantly distorted from that shown in Figure 5. However, when a depolarized pump beam is used, no distortion in the spectrum is observed near $t = 0$ even for excitation energies of several tens of microjoules. This demonstrates the need for great care in interpreting zero-time data obtained when polarized light pulses are used.

Time-Resolved Absorption Studies of the Near-IR Band of Mb. The above discussion indicate that the evolution of the CD signal results from changes in the tertiary structure of the protein. One such molecular motion that could contribute to the dynamics is the tilting of the proximal histidine. In this section, such motion is examined in detail. As discussed above, the near-IR absorption band of Mb at ≈760 nm is a porphyrin-to-iron charge-transfer transition (Iizuka et al., 1974). This band, characteristic of unliganded five-coordinate ferrous hemes, has the unique feature in that the band position is sensitive to the relative orientation of the heme and the proximal histidine. Low-temperature work by Iizka et al. (1974) showed that the near-IR band of Mb generated by photodissociation of MbCO at 4 K is significantly red shifted from the normal Mb frozen at the same temperature. The former centers at 772 nm, while the latter is at 758 nm. This spectral shift is a reflection of the unrelaxed intermediate frozen at cryogenic temperature. When the temperature is raised to ≈60 K, the intensity of the band decreases due to the geminate recombination of the CO. However, the peak position of the band also shifts to higher energy. A study by Ansari et al. (1985) attributes this spectral shift to the conformational relaxation of the protein.

Recently, Friedman and co-workers have carefully studied this spectral evolution at low temperature (Campbell et al., 1987). Their results prove that the conformation of photogenerated Mb is unrelaxed and frozen at temperatures below

60 K. Thus, the observed blue shift is not due to conformational relaxation but results from a dynamic hole-burning phenomenon associated with CO rebinding. As indicated by its Gaussian shape, the near-IR band is inhomogeneously broadened at low temperature. There is a distribution of conformational substates (Frauenfelder et al., 1988) that are trapped in local minima of the potential-energy surface. These conformational substates have slightly different spectroscopic properties as well as different ligand-rebinding kinetics. It turns out that the conformational substates at the red edge of the near-IR band have a faster rebinding rate than those at the blue edge. This results in the observed blue shift of the inhomogeneously broadened band as CO rebinding takes place. These findings provide direct evidence for the functional relevance of conformational substates in Mb (Frauenfelder et al., 1988).

At room temperature, the situation is different as 95% of CO escapes into the solvent (Henry et al., 1983). Geminate rebinding does not occur. There is rapid interconversion between different conformational substates (Elber & Karplus, 1987), and as a result the absorption band is essentially homogeneously broadened. Furthermore, the bandwidths of the absorption features, including the near-IR band, are larger at room temperature than at low temperature. In fact, the room temperature near-IR band sits on the tail of the more intense Q band. This suggests that an increased number of conformational substates are accessed with increasing temperature.

It is of great interest to know whether or not photodissociated Mb at room temperature is characterized by a shift in the maximum of the near-IR band from that found for equilibrated Mb. Such a spectral evolution would be unambiguously due to a conformational relaxation. Sassaroli and Rousseau (1987) have reported nanosecond measurements for Mb and Hb at room temperature. In photodissociated Mb, the near-IR transition has fully relaxed to its equilibrium value by 10 ns (the instrument response time of that study). In photodissociated Hb, the transition is shifted by 6 nm to longer wavelengths at 10 ns. It relaxes about halfway back to the deoxy-Hb value by about 100 ns but subsequently evolves very slowly, on a time scale of 100 ms or longer. This spectral evolution for Hb was attributed to the heme quaternary structure change, an event that takes place on a nanosecond to millisecond time scale. The absence of spectral evolution of Mb on the nanosecond time scale indicates the need for picosecond near-IR experiments. A faster (and perhaps smaller) spectral evolution of Mb is expected from the lack of quaternary structure changes and the smaller dynamic complexity of Mb as compared to Hb.

In a study of the optical properties of Hb, Eaton et al. (1978) assigned the 760-nm transition as a charge-transfer transition between the prophyrin π system aend the iron d orbital [$a_{2u}(\pi) \rightarrow d_{yz}$], polarized within the heme plane. This assignment was based on CD, MCD, single crystal polarized adsorption data, and extended Hückel calculations. A subsequent study by Makinen and Churg (1983) assigns this transition as a $d_{x2-y2} \rightarrow e_{2g}(\pi^*)$ transition on the basis of polarization data. In either case, the charge-transfer nature of this band makes it pertinent to d orbitals of iron, which are under a ligand field perturbation imposed by the surrounding protein; thus, this band is sensitive to changes in local structure.

In principle, there are two possible structural mechanisms that could give rise to a time-dependent red shift in the absorption spectra. First, changes in the properties of the iron–histidine bond would affect the energy of the iron d orbitals. In resonance Raman studies at cryogenic temperatures, it has been found that for both Hb (Olafson & Goddard, 1977; Rohmer et al., 1983) and Mb (Sassaroli et al., 1986) the iron–histidine stretching mode is shifted to higher frequency in the photoproduct as compared to the deligated form. A similar Raman shift has been observed by using 10-ns pulses to study room temperature solutions of Hb (Sassaroli et al., 1986), but no shifts were detected in Mb in 10-ns and 35-ps time-resolved experiments (Findsen et al., 1985). In the five-coordinate species, the iron moves out of plane, and the proximal histidine tilts with respect to the heme normal. The motion of the histidine causes a displacement of the F-helix (Figure 1). Therefore, the photoproduct studied under conditions in which the protein conformation is frozen and unrelaxed is an intermediate in which the iron has moved out of the heme plane but the histidine can not tilt. This intermediate has a higher iron–histidine stretching frequency. Sassaroli and Rousseau (1987) and Campbell et al. (1987) proposed that the changes in the histidine–heme orientation are also responsible for the spectral shift in the near-IR absorption band. This is consistent with the charge-transfer character of this band.

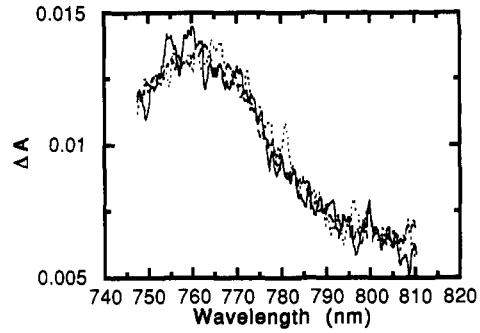

FIGURE 9: Transient near-IR absorption spectra following photodissociation of MbCO with a 0-ps (solid line), 500-ps (dotted line), and 60-ns (dashed line) time delay taken with 35-ps pump and probe pulses. No spectral evolution is observed between 35 ps and 60 ns.

Second, the near-IR spectral shift might be associated with the movement of iron out of the heme plane and/or the doming of the heme. Calculations suggest that the out-of-plane displacement of the iron results from nonbonded interactions between the proximal histidine and the pyrrole nitrogens of the heme (Olafson & Goddard, 1977; Rohmer et al., 1983). MD simulations (Henry et al., 1986) reveal that, upon the loss of CO from Mb, the iron moves out of the heme plane in 50–150 fs. Femtosecond transient absorption (Martin et al., 1983) and Raman work (Petrich et al., 1987) support this view. Nevertheless the iron motion and the heme doming might have a slow component arising from the constraints imposed by the protein immediately after photolysis. In fact, the picosecond resonance Raman work on the porphyrin skeletal modes of Mb revealed an unrelaxed heme structure at 35 ps following photolysis (Dasgupta et al., 1985). Characteristic of the C_{4v} symmetry and arising from charge transfer between the iron and the heme, the near-IR band should be sensitive to the full out-of-plane displacement of iron and the doming of the heme.

Transient difference spectra with a 0-ps, 500-ps, and 60-ns time delay following photolysis of MbCO are shown in Figure 9. Within experimental error, these spectra are all identical. These results indicate that there is not detectable spectral evolution (<2 nm) between 35 ps and 10 ns. Evolution of the near-IR band, if any, must occur within our instrumental response time. In contrast, for the related photolysis reaction of HbCO, this IR absorption band reveals a nonequilibrium spectrum on the picosecond time scale (Dunn & Simon, 1990).

These results provide evidence that following photolysis of MbCO the tilting of the proximal histidine, the dynamic displacement of iron, and the doming of the heme do not occur on a time scale longer than 30 ps. There are no changes in the near-IR absorption band on the time scale in which the CD signal varies. Therefore, neither the tilting of the proximal histidine nor the structural changes of the heme probed by the near-IR band are responsible for the observed CD kinetics.

Conclusions

In summary, through the use of time-resolved circular dichroism spectroscopy, a new relaxation process in photogenerated Mb is revealed. An extensive series of other spectroscopic experiments, including near-IR and Q-band absorption, picosecond MCD, and transient linear dichroism, have also been conducted. These complementary studies reveal no spectral evolutions on the same time scale observed in the CD experiments. This demonstrates the unique capability of transient CD spectroscopy and provides definitive evidence that the conformational relaxation of the protein requires several hundred picoseconds.

In accord with our results, recent molecular dynamics simulations show that Mb reaches its equilibrium structure with a time constant of hundreds of picoseconds following photodissociation (M. Karplus, personal communication). On the basis of the calculations of Hsu and Woody (1971), it is known that 12 aromatic amino acid residues of the protein dominate the rotational strength, some being as far away from the heme as 12 Å. The challenge that remains is to determine which of these residues are mainly responsible for the observed CD kinetics. Combined molecular dynamics simulations and CD calculations, as well as experiments on mutated Mb, would be helpful in understanding the roles of these individual residues.

It is important to note that the time scale of the conformational relaxation is competitive with the geminate recombination dynamics of Mb with ligands such as O_2, NO, and isocyanide. The role of protein conformational relaxation on the rebinding kinetics in these related systems still needs to be addressed.

Acknowledgments

We thank Hinds International for the loan of the piezoelectric modulator. We greatly appreciate the valuable discussions with Drs. William A. Eaton, Attila Szabo, and James Hofrichter and Professors Robert W. Woody and Robin Hochstrasser.

References

Alden, R. G., Ondrias, M. R., Courtney, S., Findsen, E. W., & Friedman, J. M. (1990) *J. Phys. Chem. 94*, 85–90.

Alpert, B., ElMohsni, S., Lindqvist, L., & Tfibel, F. (1979) *Chem. Phys. Lett 64*, 11–16.

Ansari, A., Berendzen, J., Bowne, S. F., Frauenfelder, H., Iben, I. E. T., Sauke, T. B., Shyamsunder, E., & Young, R. D. (1985) *Proc. Natl. Acad. Sci. U.S.A. 82*, 5000–5004.

Aojula, H. S., Wilson, M. T., Moore, G. R., & Williamson, D. J. (1988) *Biochem. J. 250*, 853–858.

Bolard, J., & Garnier, A. (1972) *Biochim. Biophys. Acta 263*, 535–549.

Brooks C. L., III, Karplus, M., & Pettitt, B. M. (1988) *Adv. Chem. Phys. 71*, 111.

Buckingham, A. D., & Stephens, P. J. (1966) *Annu. Rev. Phys. Chem. 17*, 399–433.

Campbell, B. F., Chance, M. R., & Friedman, J. L. (1987) *Science 238*, 373–376.

Case, D. A., & Karplus, M. (1979) *J. Mol. Biol. 132*, 343–368.

Chance, M. R., Courtney, S. H., Chavez, M. D., Ondrias, M. R., & Friedman, J. M. (1990) *Biochemistry 29*, 5537–5545.

Chernoff, D. A., Hochstrasser, R. M., & Steel, A. W. (1980) *Proc.Natl. Acad. Sci. U.S.A. 77*, 5606–5610.

Dasgupta, S., Spiro, T. G., Johnson, C. K., Dalickas, G. A., & Hochstrasser, R. M. (1985) *Biochemistry 24*, 5295–5297.

Duddell, D. A., Morris, R. J., & Richards, J. T. (1979) *J. Chem. Soc., Chem. Commun.*, 75–76.

Dunn, R., & Simon, J. D. (1990) *Biophys. J.* (submitted for publication).

Eaton, W. A., & Hofrichter, J. (1981) *Methods Enzymol. 76*, 175–261.

Eaton, W. A., Hanson, L. K., Stephens, P. J., Sutherland, J. C., & Dunn, J. B. R. (1978) *J. Am. Chem. Soc. 100*, 4991–5003.

Elber, R., & Karplus, M. (1987) *Science 235*, 318–321.

Findsen, E. W., Scott, T. W., Chance, M. R., & Friedman, J. M. (1985) *J. Am. Chem. Soc. 107*, 3355–3357.

Fleming, G. R. (1986) *Chemical Applications of Ultrafast Spectroscopy*, Oxford University Press, Oxford.

Frauenfelder, H., Parak, F., & Young, R. D. (1988) *Annu. Rev. Biophys. Biophys. Chem. 17*, 451.

Friedman, J. M., & Lyons, K. B. (1980) *Nature 284*, 570–572.

Genberg, L., Heisel, F., McLendon, G., & Miller, R. J. D. (1987) *J. Phys. Chem. 91*, 5521.

Genberg, L., Bao, Q., Gracewskiz, S., & Miller, R. J. D. (1989) *Chem. Phys. 31*, 81.

Gibson, Q. H. (1956) *J. Physiol. 136*, 112–122.

Goldbeck, R. A. (1988) *Acc. Chem. Res. 21*, 95–101.

Goldbeck, R. A., Dawes, T. D., Milder, S. J., Lewis, J. W., & Kliger, D. S. (1989) *Chem. Phys. Lett. 156*, 545–549.

Gouterman, M. (1961) *J. Mol. Spectrosc. 6*, 138–163.

Gouterman, M. (1978) in *The Porphyrins* (Dolphin, D., Ed.) Vol. III, pp 1–165, Academic Press, New York.

Greene, B. I., Hochstrasser, R. M., Weisman, R. B., & Eaton, W. A. (1978) *Proc. Natl. Acad. Sci. U.S.A. 75*, 5255–5259.

Henry, E. R., Sommer, J. H., Hofrichter, J., & Eaton, W. A. (1983) *J. Mol. Biol. 166*, 443–451.

Henry, E. R., Levitt, M., & Eaton, W. A. (1985) *Proc. Natl. Acad. Sci. U.S.A. 82*, 2034.

Henry, E. R., Eaton, W. A., & Hochstrasser, R. M. (1986) *Proc. Natl. Acad. Sci. U.S.A. 83*, 8982–8986.

Hochstrasser, R. M., & Johnson, C. K. (1988) in *Ultrashort Laser Pulses and Applications, Topics in Applied Physics* (Kaiser, W., Ed.) Vol. 60, pp 357–417, Springer-Verlag, New York.

Holmquist, B. (1978) in *The Porphyrins* (Dolphin, D., Ed.) Vol. III, pp 249–270, Academic Press, New York.

Hsu, M.-C. (1970) Ph.D. Thesis, University of Illinois.

Hsu, M.-C., & Woody, R. W. (1971) *J. Am. Chem. Soc. 93*, 3515–3525.

Iizuka, T., Yamamoto, H., Kontani, M., & Yonetani, T. (1974) *Biochim. Biophys. Acta 371*, 126–139.

Janes, S. M., Dalickas, G. A., Eaton, W. A., & Hochstrasser, R. M. (1988) *Biophys. J. 54*, 545–549.

Jongeward, K. A., Magde, D., Taude, D. J., Marsters, J., & Traylor, T. (1988) *J. Am. Chem. Soc. 110*, 380.

Kajiyoshi, M., & Anon, F. K. (1975) *J. Biochem. 78*, 1087–1095.

Kendrew, J. C., Dickerson, R. E., Strandberg, B. E., Hart, R. G., Davies, D. R., Phillips, D. C., & Shore, V. C (1960) *Nature 185*, 422–427.

Kirkwood, J. G. (1937) *J. Chem. Phys. 5*, 479.

Kuriyan, J., Wilz, S., Karplus, M., & Petsko, G. A. (1986) *J. Mol. Biol. 192*, 133.
La Mar, G N., Davis, N. L., Parish, D. W., & Smith, K. M. (1983) *J. Mol. Biol. 168*, 887-896.
Magde, D. (1978) *J. Chem. Phys. 68*, 3717-3734.
Makinen, M. W., & Churg, A. K. (1983) in *Iron Porphyrins* (Lever, A. B. P., & Gray, H. B., Eds.) Part 1, Chapter 3, pp 141-235, Addison Wesley, Reading, MA.
Martin, J. L., Migus, A., Poyart, C., Lecarpentier, Y., Astier, R., & Antonetti, A. (1983) *Proc. Natl. Acad. Sci. U.S.A. 80*, 173-177.
Mason, S. (1979) in *Optical Activity and Chiral Discrimination, NATO Adv. Study Inst. Ser., Ser. C 48*, 1-24.
Milder, S. J., Bjorling, S. C., Kuntz, I. D., & Kliger, D. S. (1988) *Biophys. J. 57*, 659-664.
Moore, J. N., Hansen, P. A., & Hochstrasser, R. M. (1988) *Proc. Natl. Acad. Sci. U.S.A. 85*, 5062.
Myer, Y. P., & Pande, A. (1978) *The Porphyrins* (Dolphin, D., Ed.) Vol. III, p 271, Academic Press, New York.
Olafson, B. D., & Goodard, W. A. (1977) *Proc. Natl. Acad. Sci. U.S.A. 74*, 1315.
Perrin, M. H., Gouterman, M., & Perrin, C. L. (1969) *J. Chem. Phys. 50*, 4137-4150.
Petrich, J. W., Martin, J. L., Houde, D., & Orszag, A. (1987) *Biochemistry 26*, 7914-7923.
Rohmer, M.-M., Dedieu, A., & Veilard, A. (1983) *Chem. Phys. 77*, 449.
Samejima, T., & Yang, J. T. (1964) *J. Mol. Biol. 8*, 863.
Sassaroli, M., & Rousseau, D. L. (1987) *Biochemistry 26*, 3092-3098.
Sassaroli, M., Dasgupta, S., & Rousseau, D. L. (1986) *J. Biol. Chem. 26*, 13704-13713.
Schatz, P. N., & McCaffery, A. J. (1969) *Q. Rev. Chem. Soc. 23*, 552-584.
Sharanov, Y. A., Mineyev, A. P., Livshitz, M. A., Sharonova, N. A., Zhurkin, V. B., & Lysov, Y. P. (1978) *Biochim. Biophys. Acta 4*, 139-158.
Springall, J., Stillman, M. J., & Thomson, A. J. (1976) *Biochim. Biophys. Acta 453*, 494-501.
Sutherland, J. C., & Holmquist, B. (1980) *Annu. Rev. Biophys. Bioeng. 9*, 293-326.
Sutherland, J. C., Axelrod, D., & Klein, M. P. (1971) *J. Chem. Phys. 54*, 2888-2899.
Terner, J., Spiro, T. G., Nagumo, M., Nicol, M. F., & El-Sayed, M. A. (1980) *J. Am. Chem. Soc. 102*, 3238.
Tinoco, I., Jr. (1962) *Adv. Chem. Phys. 4*, 113.
Vickery, L., Nozawa, T., & Sauer, K. (1976) *J. Am. Chem. Soc. 98*, 343.
Vikery, L. E. (1978) *Methods Enzymol. 54*, 284-302.
Woodruff, W. H., Einarsdottir, O., Dyer, R. B., Bagley, K. A., Palmer, G., Atherton, S. J., Goldbeck, R. A., Dawes, T. D., & Kliger, D. S. (1990) *J. Biol. Chem.* (submitted for publication).
Woody, R. (1978) *Biochemical and Clinical Aspects of Hemoglobin Abnormalities*, pp 279-298, Academic Press, New York.
Xie, X. (1990) Ph.D. Thesis, University of California at San Diego.
Xie, X., & Simon, J. D. (1988) *Opt. Commun. 69*, 303-307.
Xie, X., & Simon, J. D. (1989) *Rev. Sci. Instrum. 60*, 2614-2627.
Xie, X., & Simon, J. D. (1990) *J. Phys. Chem. 94*, 8014.

In Vitro Identification of Rhodopsin in the Green Alga *Chlamydomonas*†

Max Beckmann and Peter Hegemann*
Max-Planck-Institut für Biochemie, Am Klopferspitz 18a, 8033 Martinsried, Germany
Received October 23, 1990; Revised Manuscript Received January 28, 1991

ABSTRACT: The unicellular alga *Chlamydomonas* can detect both intensity and direction of the ambient light and adjust its swimming speed and direction accordingly. On the basis of physiological experiments, the functional photoreceptor for this *visual* process has recently shown to be a rhodopsin. We here report the in vitro identification of endogenous retinal and a rhodopsin in *Chlamydomonas* cell extracts and purified membrane preparations. The rhodopsin absorption spectrum has fine structure with the maximum at 495 nm and matches the action spectra for the behavioral light responses. The rhodopsin can be bleached and subsequently reconstituted with exogenous retinal. Labeling with [^{3}H]retinal occurs in the final preparation only with a single protein with a molecular weight of 32 000. We conclude that this protein is the visual photoreceptor in *Chlamydomonas*.

The unicellular alga *Chlamydomonas* can use light as an energy source (photosynthesis), as a regulator for developmental processes (photomorphogenesis), and as a sensory stimulus for orientation to or away from a light source (phototaxis and stop responses; Pfeffer, 1904; Schmidt & Eckert, 1976; Foster & Smyth, 1980; Nultsch & Häder, 1988; Hegemann & Bruck, 1988). While the photoreceptors for photosynthesis and photomorphogenesis, e.g., reaction centers and phytochrome, have been studied extensively for many years, the photoreceptor for behavioral light responses has only recently been dealt with. Phototaxis and light-induced stop responses of *Chlamydomonas reinhardtii* show rhodopsin action spectra and are retinal dependent (Foster et al., 1984; Uhl & Hegemann, 1990). Retinal can restore phototaxis in

† This work was supported by the Deutsche Forschungsgemeinschaft (P.H.).
* Address correspondence to this author.

0006-2960/91/0430-3692$02.50/0